

## Supplementary Information

### **MOF-derived PdNiCo alloys encapsulated in nitrogen-doped graphene for robust hydrogen evolution reactions**

Shihao Xu,<sup>a,b</sup> Fan Yang,<sup>a,b</sup> Shuai Han,<sup>a,b</sup> Shudong Zhang,<sup>\*a,c</sup> Qiang Wang,<sup>\*d,e</sup> and Changlong Jiang<sup>\*a,c</sup>

<sup>a</sup> Institute of Solid State Physics, Hefei Institutes of Physical Science, Chinese Academy of Sciences, Hefei, Anhui, 230031, China.

<sup>b</sup> Department of Chemistry, University of Science and Technology of China, Hefei, Anhui 230026, China.

<sup>c</sup> Key Laboratory of Photovoltaic and Energy Conservation Materials, Hefei Institutes of Physical Science, Chinese Academy of Sciences, Hefei, Anhui, 230031, China.

<sup>d</sup> Jiangsu Collaborative Innovation Centre of Photovoltaic Science and Engineering, Changzhou University, Changzhou, Jiangsu, 213164, China.

<sup>e</sup> School of Materials Science and Engineering, Changzhou University, 213164, P.R. China.

\* Corresponding authors.

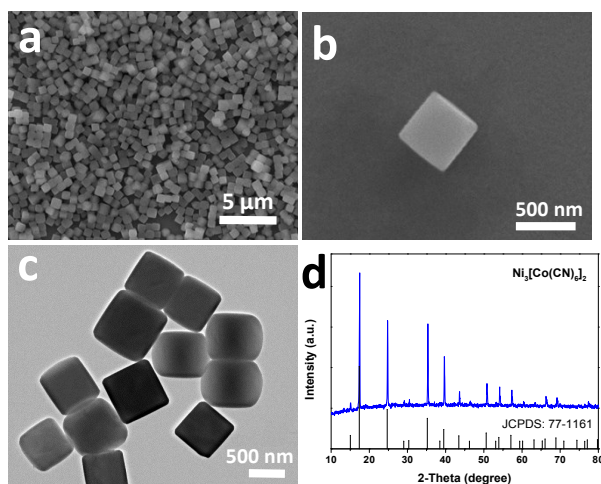


**Fig. S1** The as-prepared  $\text{Ni}_3[\text{Co}(\text{CN})_6]_2$  MOF precursor particles. (a,b,c) FESEM and TEM images of the as-prepared  $\text{Ni}_3[\text{Co}(\text{CN})_6]_2$  MOF precursor particles. (d) The XRD result of the as-prepared  $\text{Ni}_3[\text{Co}(\text{CN})_6]_2$  MOF precursor particles.

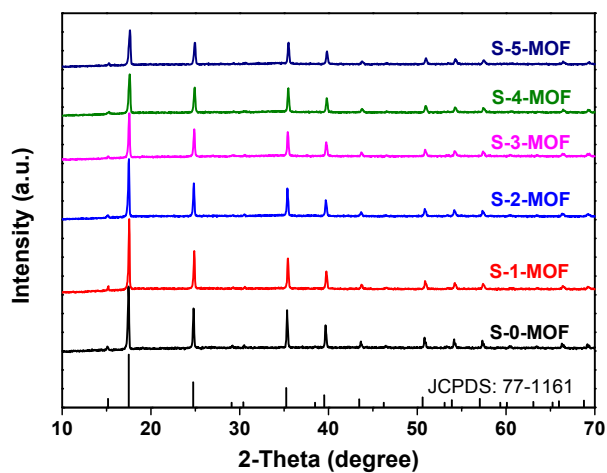


**Fig. S2** The X-ray diffraction patterns of S-0-MOF, S-1-MOF, S-2-MOF, S-3-MOF, S-4-MOF and S-5-MOF.

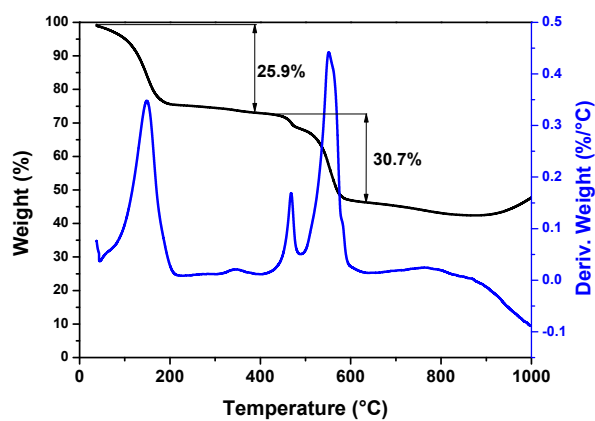


**Fig. S3** The TG curve of as-prepared  $\text{Ni}_3[\text{Co}(\text{CN})_6]_2$  precursor.

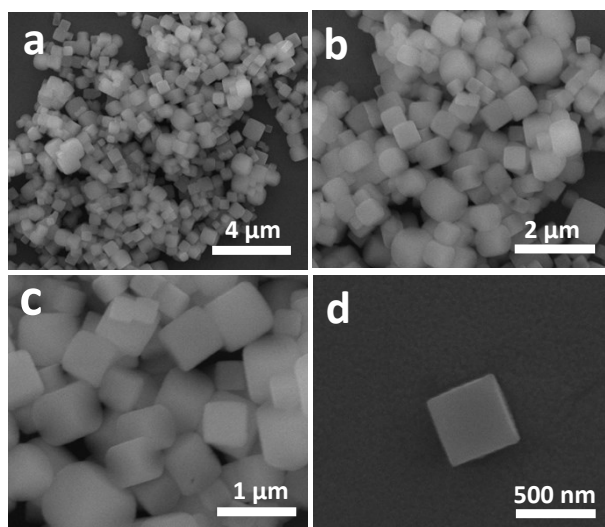


**Fig. S4** SEM images of as-prepared Pd-doped  $\text{Ni}_3[\text{Co}(\text{CN})_6]_2$  precursor at different magnifications.

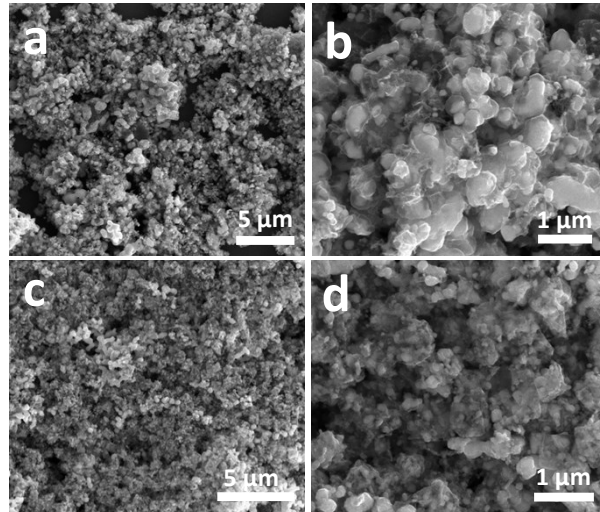


**Fig. S5** SEM images of S-0 (a,b) and S-1(c,d).

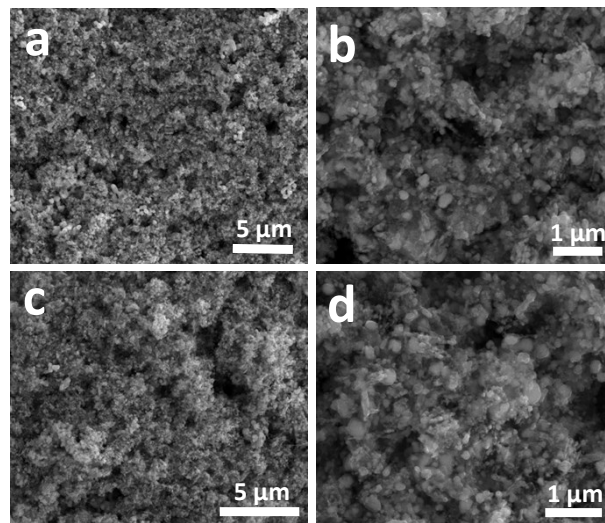


**Fig. S6** SEM images of S-2 (a,b) and S-3(c,d).

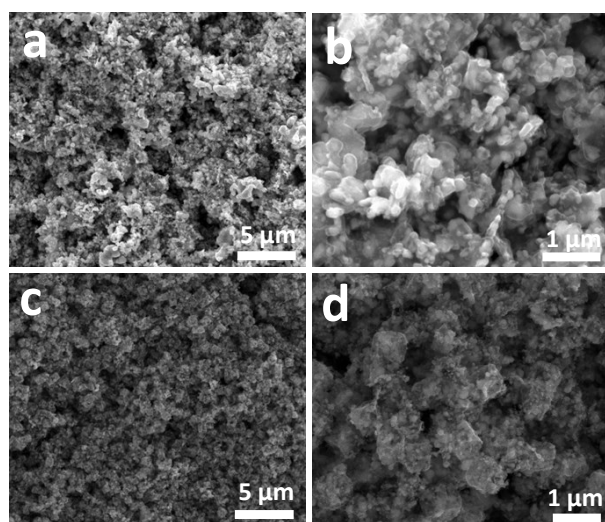


**Fig. S7** SEM images of S-2 (a,b) and S-3(c,d).

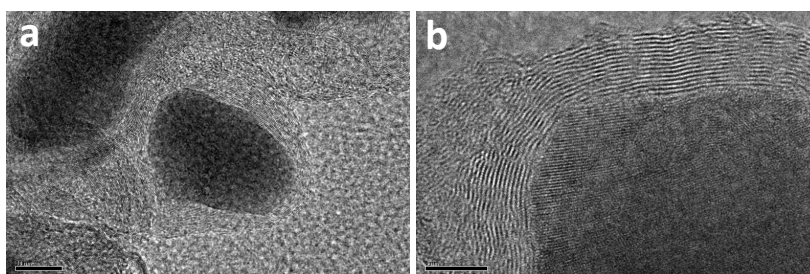


**Fig. S8** TEM images of S-5.

**Table S1.** Various N atoms percentages of different samples from XPS results.

Sample	Pyridinic-N (%)	Pyrrolic-N (%)	Graphitic-N (%)	Total N content in different sample (%)
S-0	33.0	34.2	32.8	5.91
S-1	33.2	34.1	32.7	9.54
S-2	33.6	33.9	32.5	10.8
S-3	33.7	33.6	32.7	10.1
S-4	33.9	32.9	33.2	13.8
S-5	33.6	33.6	32.8	8.4

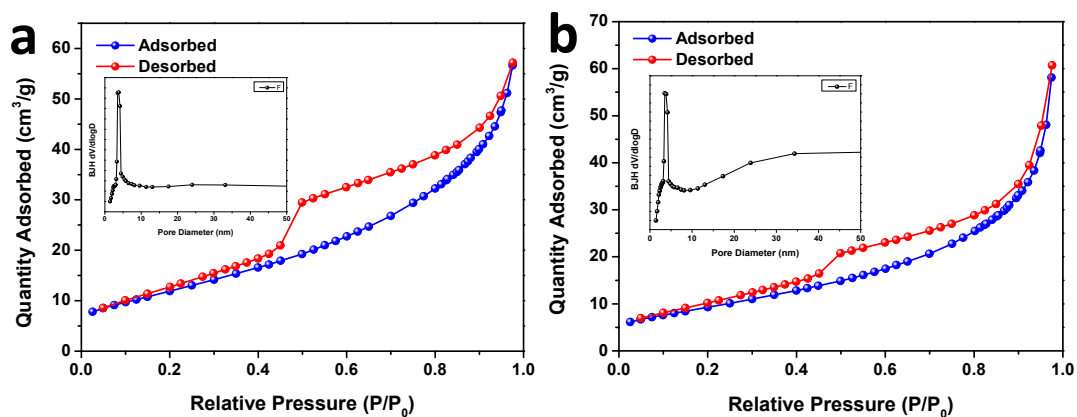


**Fig. S9** Nitrogen adsorption-desorption isotherm and the corresponding BJH pore size distribution of S-4 (a) and S-5 (b).

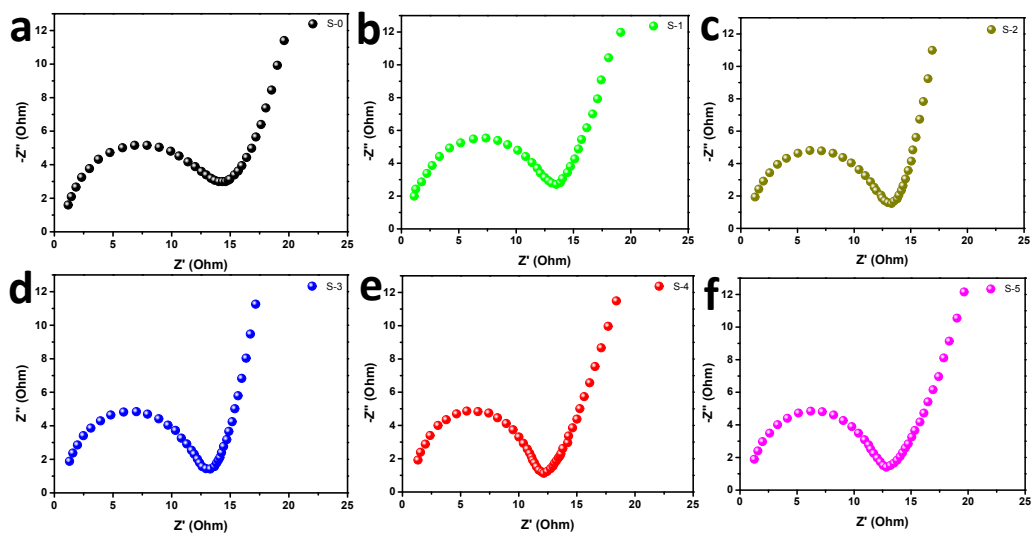


**Fig. S10** Electrochemical impedance spectroscopy (EIS) Nyquist plots for S-0, S-1, S-2, S-3, S-4 and S-5 collected in frequency range of  $1-10^5$  Hz in 1 M KOH electrolyte.

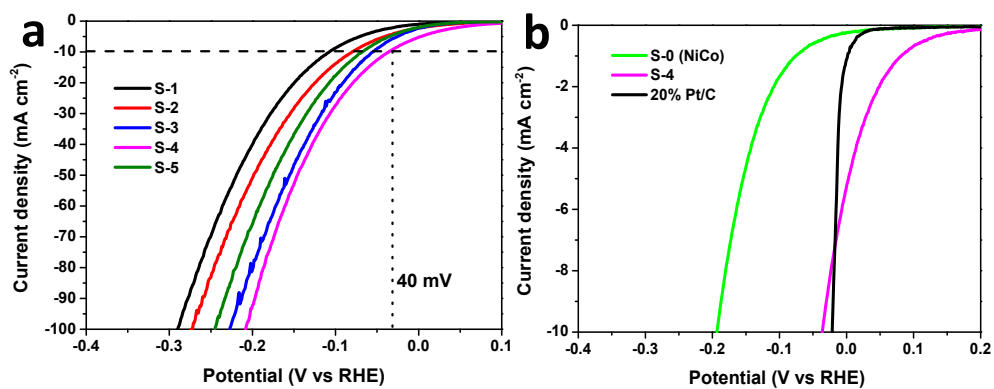


**Fig. S11** The polarization curves of the as-prepared PdNiCo@NC samples (vs. RHE) in  $N_2$  saturated 0.5 M  $H_2SO_4$  solution.

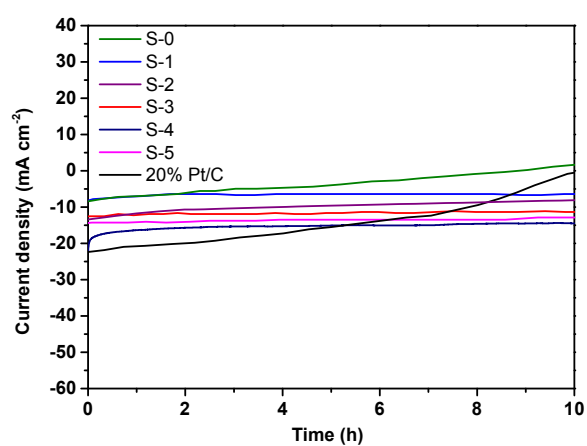


**Fig. S12** Chronoamperometry current density curve (i-t curve) for Pt/C catalyst and PdNiCo@NC samples under static overpotential of 70 mV vs. RHE for 10 h in 1 M KOH electrolyte.

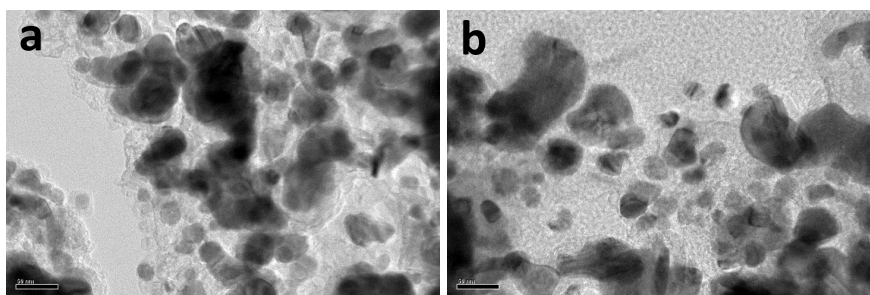


**Fig. S13** TEM images of S-4 (a) and S-5(b) after cycling experiment.